Biotechnology for Biofuels and Bioproducts

RESEARCH

Open Access

Furfural tolerance of mutant *Saccharomyces cerevisiae* selected via ionizing radiation combined with adaptive laboratory evolution

Junle Ren[1,2†], Miaomiao Zhang[1,2†], Xiaopeng Guo[3*], Xiang Zhou[1,2], Nan Ding[1,2], Cairong Lei[1,2], Chenglin Jia[1,2], Yajuan Wang[1,2], Jingru Zhao[1,2], Ziyi Dong[1,2] and Dong Lu[1,2*]

Abstract

Background Lignocellulose is a renewable and sustainable resource used to produce second-generation biofuel ethanol to cope with the resource and energy crisis. Furfural is the most toxic inhibitor of *Saccharomyces cerevisiae* cells produced during lignocellulose treatment, and can reduce the ability of *S. cerevisiae* to utilize lignocellulose, resulting in low bioethanol yield. In this study, multiple rounds of progressive ionizing radiation was combined with adaptive laboratory evolution to improve the furfural tolerance of *S. cerevisiae* and increase the yield of ethanol.

Results In this study, the strategy of multiple rounds of progressive X-ray radiation combined with adaptive laboratory evolution significantly improved the furfural tolerance of brewing yeast. After four rounds of experiments, four mutant strains resistant to high concentrations of furfural were obtained (SCF-R1, SCF-R2, SCF-R3, and SCF-R4), with furfural tolerance concentrations of 4.0, 4.2, 4.4, and 4.5 g/L, respectively. Among them, the mutant strain SCF-R4 obtained in the fourth round of radiation had a cellular malondialdehyde content of 49.11 nmol/mg after 3 h of furfural stress, a weakening trend in mitochondrial membrane potential collapse, a decrease in accumulated reactive oxygen species, and a cell death rate of 12.60%, showing better cell membrane integrity, stable mitochondrial function, and an improved ability to limit reactive oxygen species production compared to the other mutant strains and the wild-type strain. In a fermentation medium containing 3.5 g/L furfural, the growth lag phase of the SCF-R4 mutant strain was shortened, and its growth ability significantly improved. After 96 h of fermentation, the ethanol production of the mutant strain SCF-R4 was 1.86 times that of the wild-type, indicating that with an increase in the number of irradiation rounds, the furfural tolerance of the mutant strain SCF-R4 was effectively enhanced. In addition, through genome-transcriptome analysis, potential sites related to furfural detoxification were identified, including *GAL7*, *MAE1*, *PDC6*, *HXT1*, *AUS1*, and *TPK3*.

Conclusions These results indicate that multiple rounds of progressive X-ray radiation combined with adaptive laboratory evolution is an effective mutagenic strategy for obtaining furfural-tolerant mutants and that it has the potential to tap genes related to the furfural detoxification mechanism.

[†]Junle Ren and Miaomiao Zhang have contributed equally to this work and should be considered co-first authors.

*Correspondence:
Xiaopeng Guo
guoxp@lut.edu.cn
Dong Lu
ld@impcas.ac.cn
Full list of author information is available at the end of the article

Highlights

- Multi-round progressive X-ray radiation combined ALE bred furfural-resistant mutants
- Mutants obtained through four rounds of radiation exhibited higher resistance to furfural
- Membrane integrity, stable mitochondrial function, and antioxidant capacity, played an important role in resisting furfural stress
- Multi-omics analysis identified many potential mutational sites that enhance the strain's furfural tolerance

Keywords Furfural, Second generation biofuel ethanol, Evolution, Whole genome resequencing, *Saccharomyces cerevisiae*

Graphical Abstract

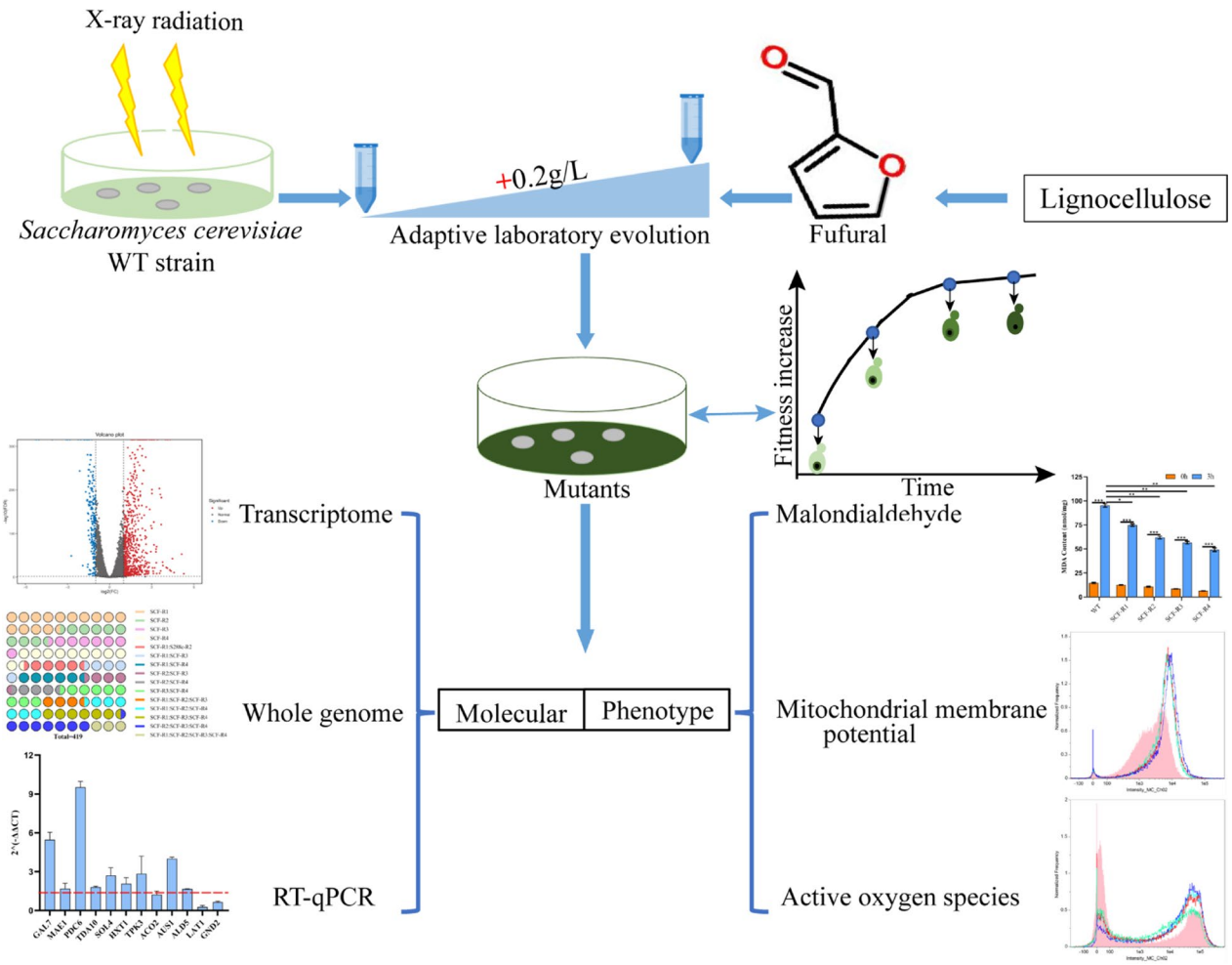

Background

As the world experiences a worsening energy crisis, ethanol is garnering recognition as a second-generation biofuel [1] and is projected to become the most important carbon–neutral resource for reducing CO_2 emissions [2]. Lignocellulosic biomass is a promising renewable resource, and is considered an excellent source of sugars for microbial conversion, especially for ethanol production [3]. However, lignocellulosic biomass pretreatment always generates fermentation inhibitors, such as furan aldehydes (furfural, 5-hydroxymethyl furfural, etc.), phenolics (vanillin, syringaldehyde, etc.), and weak acids (formic acid, acetic acid, etc.) [4]. In particular, furfural is a strongly cytotoxic product of pentose dehydration during lignocellulosic hydrolysis [5], restricting *Saccharomyces cerevisiae* growth, metabolism, ethanol production, cell morphology, and physiological status [6–8]. Furfural severely inhibits intracellular redox metabolism and induces the accumulation of reactive oxygen species, thus damaging the mitochondria, endoplasmic reticulum, membrane integrity, actin cytoskeleton, and nuclear chromatin [7, 8]. Furfural also affects adenosine triphosphate (ATP) production rates and RNA/protein synthesis [9, 10]. Therefore, a top priority in sustainable energy production is addressing the negative effect of hazardous chemicals on microorganisms. Shui et al. [11] obtained four *Zymomonas mobilis* mutants tolerant to furfural stress through adaptive laboratory evolution, with a furfural tolerance level of 3.0 g/L. Luo et al. [12] introduced the *irrE* gene from radiation-resistant bacteria into brewing yeast to generate a mutant with furfural tolerance at 2.0 g/L. Huang et al. [13] obtained a *Z. mobilis* mutant tolerant to 3.0 g/L furfural through PCR-based whole-genome recombination. However, the concentration of aldehydes in lignocellulosic hydrolysate ranges from 2.0 to 5.9 g/L [10]. At present, the industry is relying on increasing the tolerance of microorganisms to toxic compounds, but existing methods are limited in their capacity to improve resistance. Therefore, a new strategy is urgently needed to develop mutant microbial strains that can tolerate high concentrations of hazardous chemicals while efficiently converting ethanol.

Ionizing radiation is a potential solution because of its wide mutation spectrum and high mutation efficiency [14]. Mutant strains obtained via ionizing radiation are better able to withstand the adverse effects of dangerous substances [15, 16]. Hence, multi-round progressive radiation based on ionizing radiation was recently developed as a novel form of microbial breeding. A notable advantage of the technique is the ability to screen for different targets in each round, thus enhancing comprehensive performance and overall species quality [17]. The wild-type (WT) strain is first irradiated to obtain a mutant with target traits that is then used as the strain for the next round of irradiation. Multi-round progressive radiation is now widely applied in microbial breeding [17]. For example, irradiating *Clostridium tyrobutyrate* with two rounds of carbon ion beams yielded a mutant that produced more organic acids under extremely acidic environmental stress [18]. One round of nitrogen ion beam implantation was sufficient to obtain an *S. cerevisiae* mutant with a high biomass and ethanol fermentation ability, and six rounds screened out a heat-resistant mutant with the characteristics of high biomass, high ethanol fermentation ability, and high-temperature resistance [19]. Finally, five rounds of low-energy nitrogen ion irradiation of an attenuator *Bacillus* resulted in a mutant with propylamine tolerance and a 2.54-fold increase in the EC_{50} value [20]. In summary, multiple rounds of progressive radiation can enhance a variety of desired traits. However, progressive radiation still has many shortcomings as applied to microbial breeding, including random and non-directional mutations, the heavy workload involved in screening, and the inability to accurately locate target mutants.

One way to address these shortcomings is through adaptive laboratory evolution (ALE), also known as evolutionary engineering. This concept takes advantage of phenotypic plasticity and flexibility in response to adverse environmental conditions (such as ethanol, high sugar, toxic compounds, and other stressors) [21–24]. In most environments, mutants are generally neutral, and when non-neutral mutations occur, they tend to be harmful rather than beneficial. However, during ALE, selected microorganisms are continuously cultured under specific stress conditions to produce improved phenotypes [25, 26]. Experiments using this method have successfully eliminated harmful mutations and increased beneficial mutations in the new population [27], including single nucleotide polymorphisms (SNPs) and small-scale DNA insertions and deletions (InDels) [28, 29]. This selective pressure eventually leads to directional evolution that improves a strain's characteristics, generating mutants with a high growth rate, high lipid content, tolerance to toxic compounds, or the ability to survive under extreme environmental conditions [30]. Other ALE experiments have successfully selected for the strains most suitable for further breeding that are rich in favorable new mutations [31]. Research focusing specifically on ethanol resistance [22] have used ALE to obtain mutants with a higher specific growth rate and specific ethanol production rate than WT under ethanol stress. Finally, ALE studies aiming to increase the ethanol

yield of xylose fermentation strains [23, 24] were able to increase both the xylose utilization rate by 1.65-fold [24] and the ethanol yield by 22.9% [23]. While these enhancements are promising, deriving high-performance strains with ALE is time-intensive, and the new strains often lack genetic stability. This requires researchers to combine ALE with innovative approaches and advanced technologies, such as radiation mutagenesis breeding [32] and high-throughput screening [33], to decouple beneficial mutations, thereby reducing the potential drawbacks of laboratory evolution experiments.

In this study, multiple rounds of progressive X-ray irradiation were combined with ALE to efficiently breed a dominant mutant of *S. cerevisiae* that can tolerate high-concentration furfural stress. The genetic information of the obtained positive mutants was revealed through multi-omics joint analysis, and new genes related to furfural toxicity were identified. The results of this study provide a new strategy to breed *S. cerevisiae* mutants with greater lignocellulose utilization efficiency and a larger ethanol yield. An improved *S. cerevisiae* strain is a valuable solution to the issues of energy security and global warming.

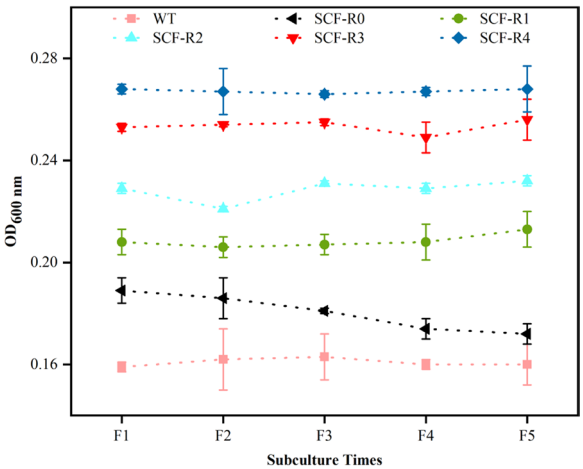

Fig. 1 Evaluation of the growth stability of the strains. WT: wild-type strain; SCF-R0: strain screened by adaptive laboratory evolution; SCF-R1: mutant strain obtained by the first round of radiation plus furfural domestication; SCF-R2: mutant strain obtained by the second round of radiation and furfural domestication; SCF-R3: mutant strain obtained by the third round of radiation plus furfural domestication; SCF-R4: mutant strain obtained by the fourth round of radiation plus furfural domestication. The results shown are the average of the three experiments

Results

Screening of furfural-resistant mutants using multi-round X-ray progressive radiation plus ALE

Four mutants (SCF-R1, SCF-R2, SCF-R3, and SCF-R4) and one WT strain (SCF-R0) were obtained. SCF-R1, SCF-R2, SCF-R3, and SCF-R4 tolerated 4.0, 4.2, 4.4, and 4.5 g/L furfural, respectively, whereas SCF-R0 tolerated only 3.5 g/L furfural. Next, the growth stability of these five strains was tested under furfural stress for five consecutive generations. The four mutants exhibited strong growth stability, with their furfural stress tolerance ranked in the following order: SCF-R4 > SCF-R3 > SCF-R2 > SCF-R1 (Fig. 1). In contrast, SCF-R0 degenerated by the fourth generation, and its growth stability was poor.

Growth performance of mutant strains under furfural stress

In solid yeast extract peptone dextrose (YPD) medium containing furfural, mutant SCF-R4 was better able to tolerate furfural stress than the other three mutants, while all four mutants tolerated furfural stress better than the WT strain (Fig. 2a). In the YPD medium containing 3.5 g/L furfural, mutant SCF-R4 had an $OD_{600} = 0.279$ at 48 h, and a growth rate that was 1.45, 1.53, 1.56, and 2.18 times faster than the growth rates of mutants SCF-R3, SCF-R2, SCF-R1, and WT SCF-R0, respectively (Fig. 2b). After being under stress for 36 h, mutant SCF-R4 began to grow, while the other mutants remained in the lag stage for another 12 h; the WT strain had a far longer lag time of 72 h (twice the duration of SCF-R4) (Fig. 2b). The specific growth rates of SCF-R4, SCF-R3, SCF-R2, and SCF-R1 were 0.036, 0.017, 0.012, and 0.011 h^{-1}, respectively, whereas the WT growth rate was 0.004 h^{-1}. In summary, the SCF-R4 mutant, obtained after the fourth round of irradiation, was the least affected by furfural toxicity.

Intracellular malondialdehyde and mitochondrial membrane potential of mutant strains after furfural stress

After 3 h of furfural stress, the malondialdehyde (MDA) content increased significantly from the levels at 0 h in all five strains (four mutants and WT; Fig. 3a), indicating the occurrence of lipid peroxidation. Specifically, the WT MDA content was 95.20 nmol/mg, which was 1.94, 1.69, 1.55, and 1.27 times higher than the MDA content of SCF-R4, SCF-R3, SCF-R2, and SCF-R1, respectively. Therefore, the four mutants had stronger lipid peroxidation resistance than the wild-type; the mutant SCF-R4 had an MDA content of 49.11 nmol/mg, significantly lower than those of the other mutants and the WT strain, indicating its superior performance in alleviating oxidative stress damage.

The mitochondrial membrane potential (MMP) change trend of all five strains after furfural stress for 0 h were identical, but at 3 h, the MMP began to shift downward (Fig. 3b, c). Notably, the WT strain exhibited stronger change than the four mutant strains, indicating that the

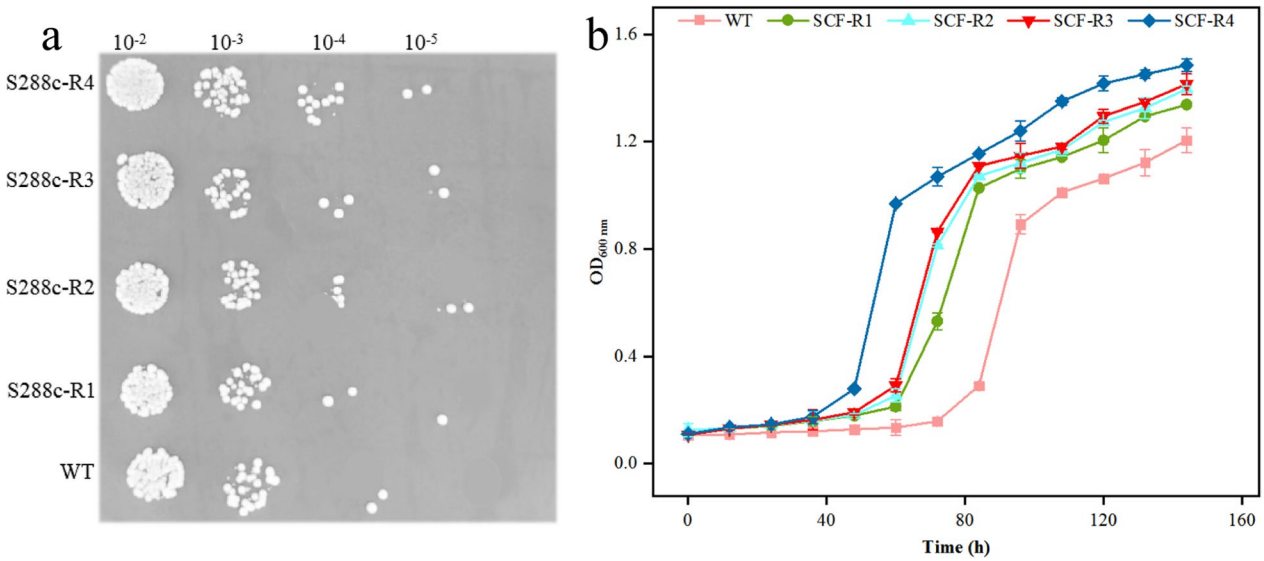

Fig. 2 Performance of the *Saccharomyces cerevisiae* mutant strains and WT strain tolerant to high-concentration furfural stress. **A** The furfural tolerance of the four mutant strains and WT strain was observed by plate dot; **B** growth curves of the mutant and wild-type strains in YPD medium containing 3.5 g/L furfural. The results shown are the average of the three experiments. WT, wild-type; YPD, yeast extract peptone dextrose

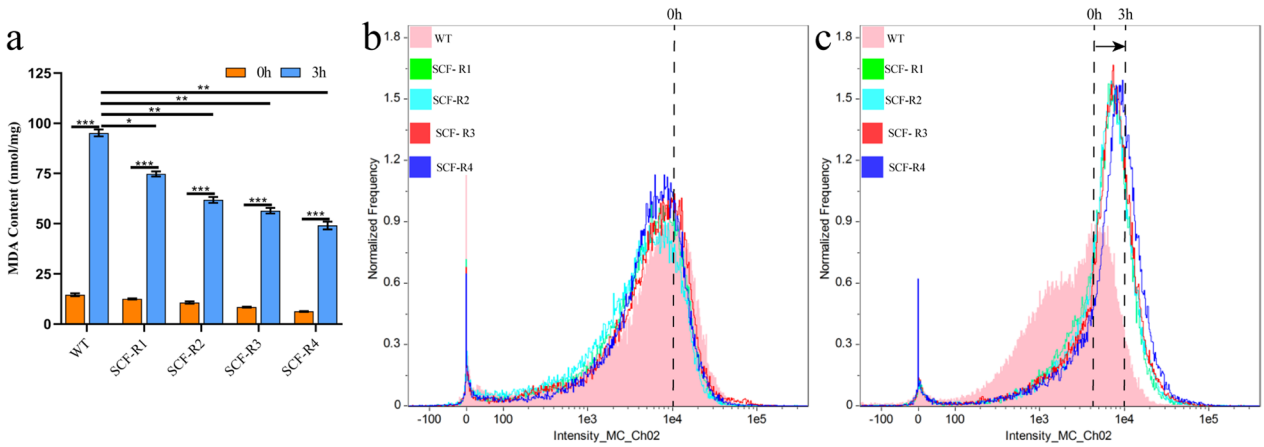

Fig. 3 Changes in the intracellular MDA and mitochondrial membrane potential of four mutant strains and the WT strain under furfural stress. **a** Intracellular MDA content of the four mutant strains and WT strain under furfural stress at 0 and 3 h (the results shown are the average of the three experiments); **b** and **c** changes in the intracellular MMP of four mutant strains and the WT strain under furfural stress at 0 and 3 h. MDA, malondialdehyde; WT, wild-type; MMP, mitochondrial membrane potential

mutants had an advantage in maintaining MMP stability under furfural stress (Fig. 3c).

Intracellular reactive oxygen species in mutant strains after furfural stress

In solid YPD medium containing 1.0 mmol/L hydrogen peroxide, the mutant strains grew better than WT, while mutant SCF-R4 was superior to mutants SCF-R3, SCF-R2, and SCF-R1 (Fig. 4a). Additionally, the results of 2,7-dichlorodihydrofluorescein diacetate (DCFH-DA) evaluation (Fig. 4b, c) showed that 3 h of furfural stress increased reactive oxygen species (ROS) in all five strains during cell growth (Fig. 4c).

A second peak was observed in the − 100 to 100 range (Fig. 4c), indicating that furfural stress was sufficient to damage the internal cellular structure and cause cell death. Therefore, the number of cells was counted during this interval. After 3 h of furfural stress, the WT death rate was 48.70%, whereas the death rates of mutants SCF-R1, SCF-R2, SCF-R3, and SCF-R4 were 23.40%,

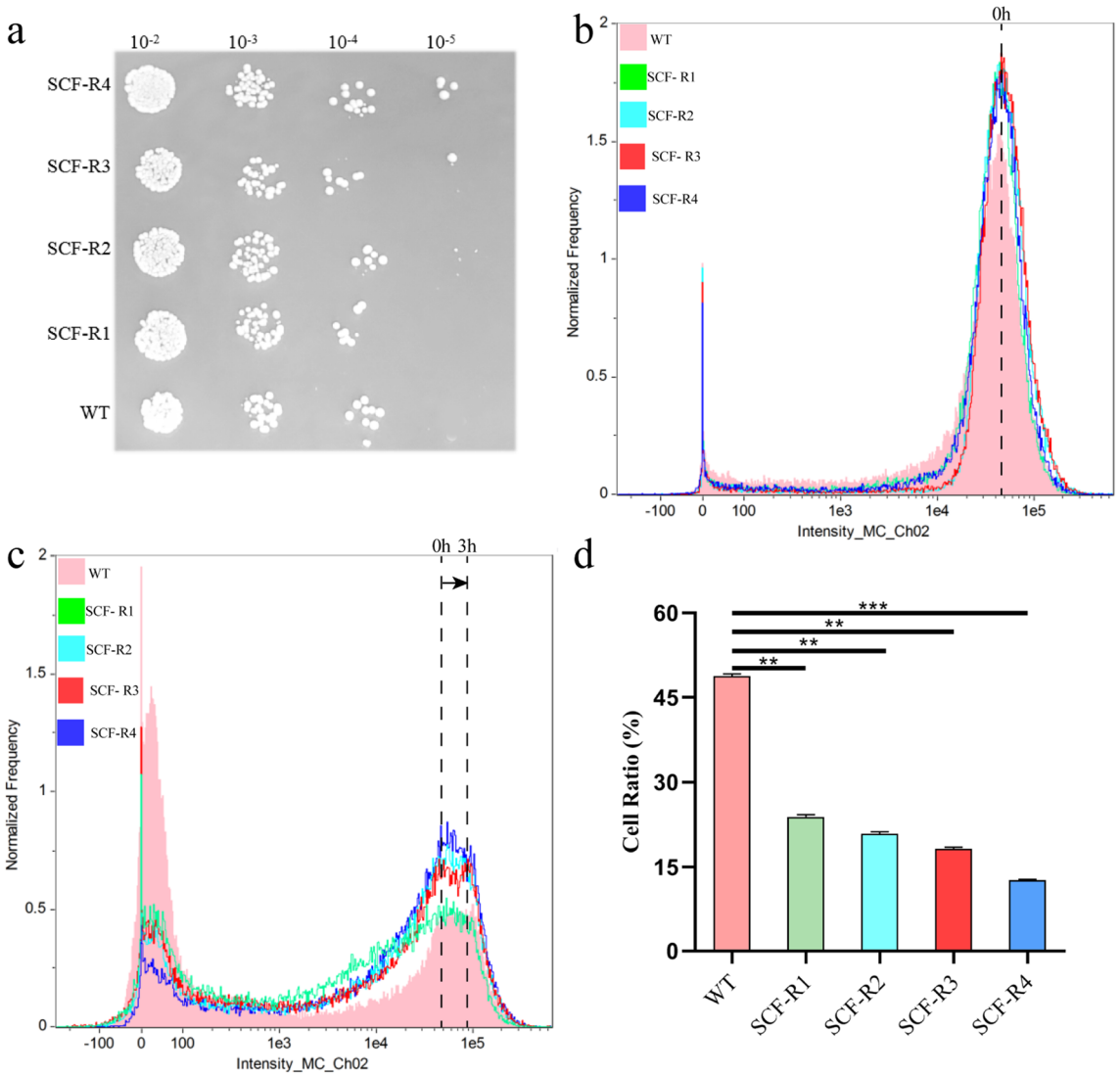

Fig. 4 Analysis of changes in ROS in *Saccharomyces cerevisiae* cells under furfural stress via flow cytometry. **a** The growth ability of the four mutant strains and WT strain under 1.0 mmol/L hydrogen peroxide stress; **b** and **c** change in the ROS in the cells of the four mutant strains and WT strain under furfural stress at 0 and 3 h; **d** the proportion of dead cells in the four mutant strains and WT strain under furfural stress for 3 h. The results shown are the average of the three experiments. ROS, reactive oxygen species; WT, wild-type

20.80%, 18.1%, and 12.60%, respectively (Fig. 4d). The difference between WT and the mutants was significant, and mutant SCF-R4 had the fewest dead cells among all the mutants. Overall, SCF-R4 was significantly more resistant to furfural-induced oxidative damage than WT or the other mutant strains.

Transcriptome profiles after furfural stress

Transcription profiles from three untreated and three furfural-treated cell samples. A total of 2156 differentially expressed genes (DEGs) (1110 up-regulated and 1046 down-regulated) (Fig. 5a) were identified and subjected to Kyoto Encyclopedia of Genes and Genomes (KEGG) enrichment analysis, with the following thresholds: enrichment factor ≥ 2 and q-value ≤ 0.01 (Fig. 5c, d). The results revealed that after furfural stress, 89 up-regulated DEGs were enriched in the ribosomal pathway and 51 were enriched in eukaryotic ribosomal biogenesis, suggesting an important role of ribosomes. Furthermore, 23 DEGs were enriched in the RNA polymerase pathway. Among the down-regulated genes, 261 DEGs were related to various metabolic pathways, 12 to autophagy pathways, 17 to longevity regulation, 28 to yeast phagocytosis, and 16 to peroxisome pathways.

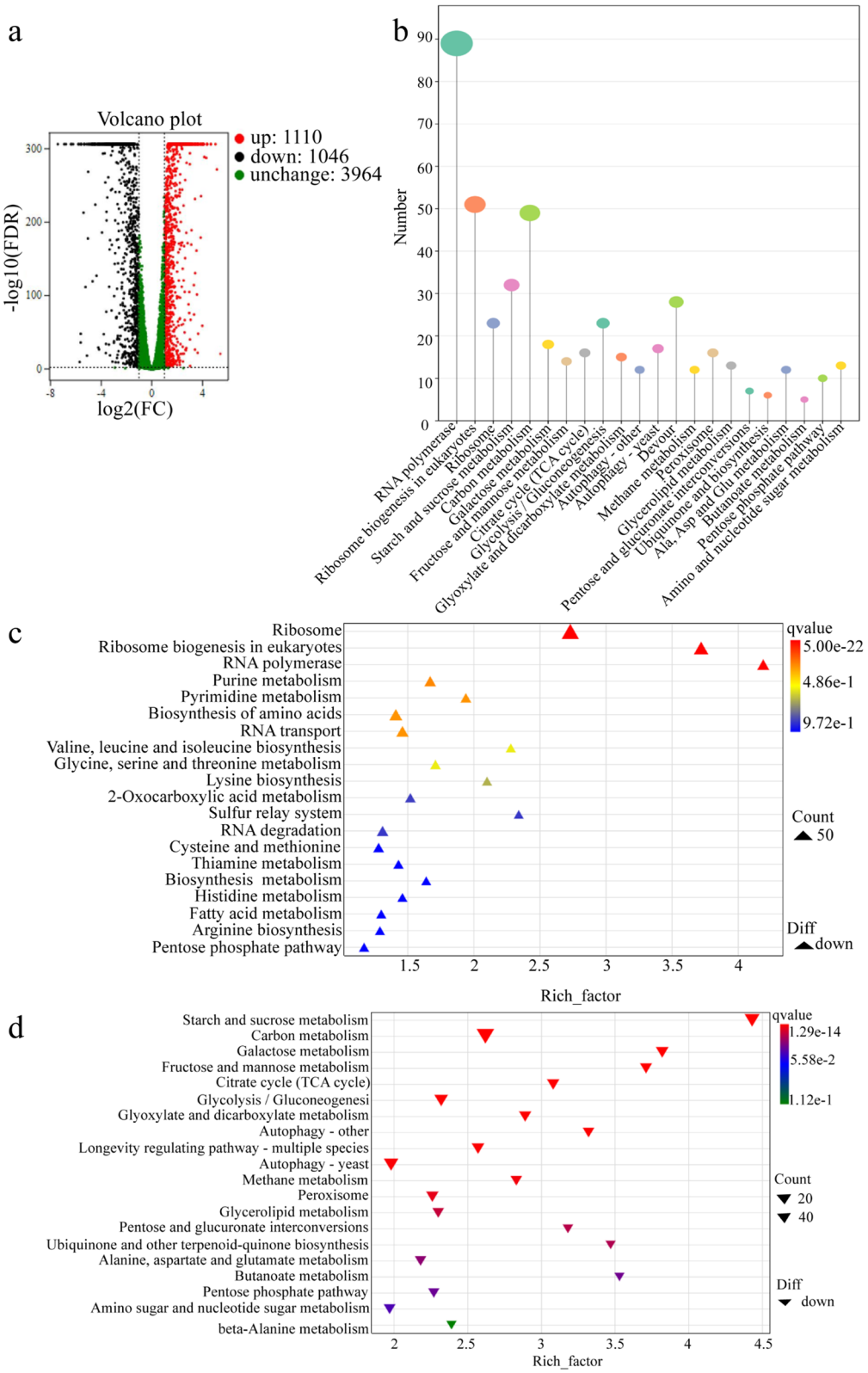

Fig. 5 Analysis of the transcriptome data of *Saccharomyces cerevisiae* under furfural stress. **a** Volcanic map of differentially expressed genes; **b** DEG statistics in each pathway; **c** and **d** KEGG enrichment map of up-regulated and down-regulated genes under furfural stress. DEG, differentially expressed genes; KEGG, Kyoto Encyclopedia of Genes and Genomes

Thus, furfural stress appears to inhibit these pathways in *S. cerevisiae* (Fig. 5b).

A total of 140 up-regulated genes and 300 down-regulated genes that met the threshold conditions were identified in these pathways. After furfural addition, genes related to ribosome synthesis were up-regulated, and 20 genes related to ribosome function were within the threshold (Schedule 1). Moreover, 50 genes ($|\log2(\text{fold change})| \geq 2$ and false discovery rate ≤ 0.01) were related to carbohydrate metabolism after furfural stress (Schedule 2), suggesting that the ability of *S. cerevisiae* to utilize carbon sources decreased under furfural stress.

Whole genome resequencing data of mutant strains

To clarify the mechanism underlying improved furfural tolerance, the whole genomes of the four mutant strains were resequenced for comparison with the WT genome. The lack of spontaneous mutations was verified by subjecting the WT strain to the same number of subcultures and the same conditions as the mutant strains. SCF-R1, SCF-R2, SCF-R3, and SCF-R4 had 41, 45, 36, and 37 SNPs, respectively, as well as 177, 155, 158, and 187 InDels (Fig. 6a), totaling 218, 200, 194, and 224 mutation sites. The mutation frequencies per site of SCF-R1, SCF-R2, SCF-R3, and SCF-R4 were

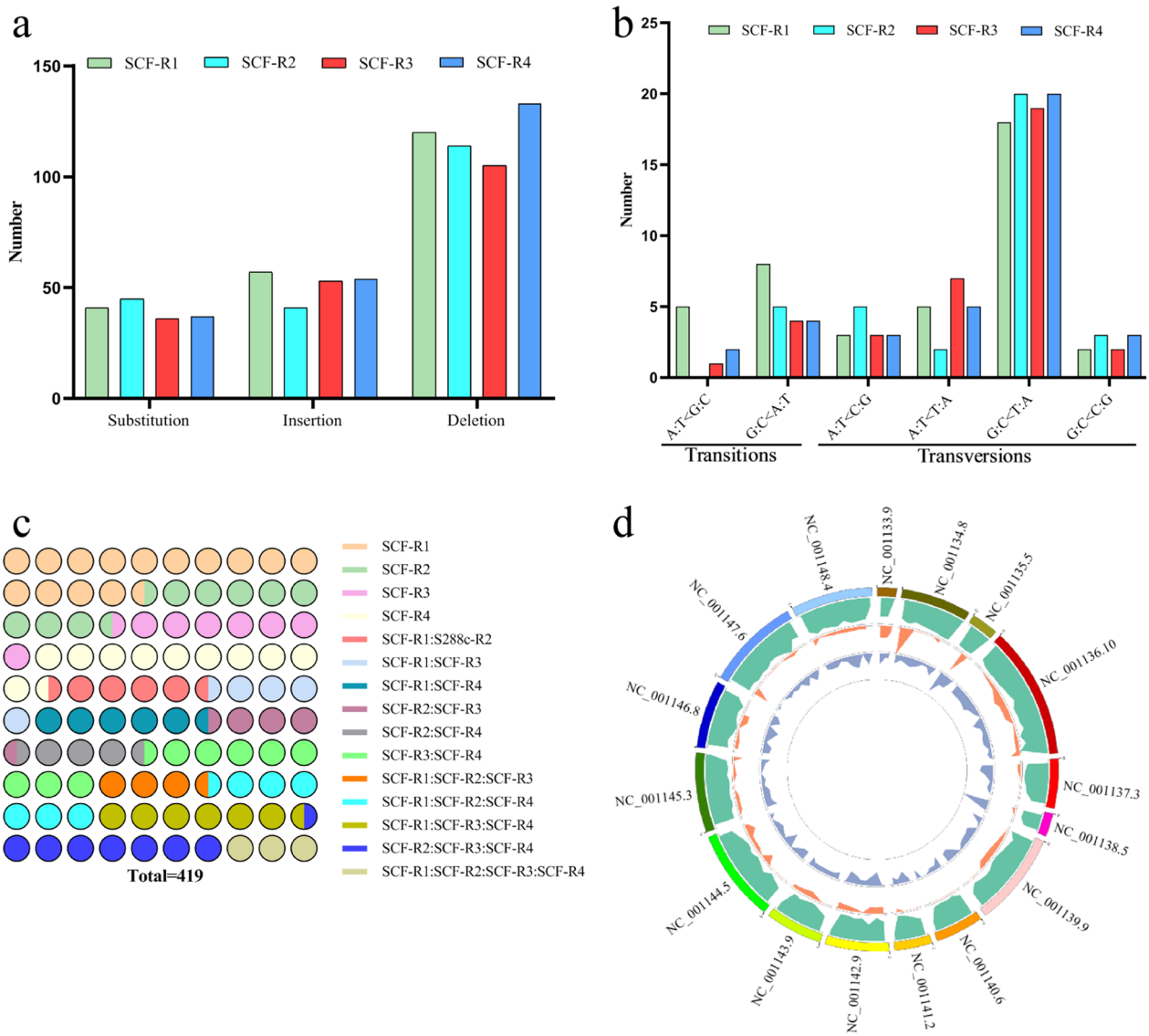

Fig. 6 Analysis of mutant genome data. **a** Statistics of various mutation types; **b** conversion and transversion ratio of single base substitution; **c** chromosome distribution of four furfural-resistant mutants and genomic mutations; the change from one base sequence (a) to another base sequence (b) is represented by a–b; **d** statistics of mutation sites

1.82×10^{-5}, 1.67×10^{-5}, 1.62×10^{-5}, and 1.87×10^{-5}, respectively.

The calculated potential spontaneous mutation frequency was 1.75×10^{-9} [34], and the spontaneous mutation frequency of small InDels per passage was much lower than the actual mutation frequency in the mutant nuclear genome. Additionally, the treatment-induced mutation rates were dominant to the spontaneous mutation rates. The base conversion and base transversion ratios of mutant strains SCF-R1, SCF-R2, SCF-R3, and SCF-R4 were 0.464, 0.194, 0.167, and 0.129, respectively, all less than 1 (Fig. 6b). Generally, Ti/Tv < 1 [35] in induced mutations, consistent with the findings of this study. As the radiation time increased, Ti/Tv gradually decreased, further demonstrating that the mutation sites in the mutant strains originated from the treatment and not from spontaneous mutation.

In total, 419 mutation sites (Fig. 6c) were identified, distributed across 17 chromosomes of *S. cerevisiae* (Fig. 6d). The InDels were mainly 1–2 bp, although larger InDels were also present, including a 29-bp insertion in mutant SCF-R1, as well as 45- and 97-bp deletions; a 45-bp insertion in SCF-R2; and a 45-bp insertion in SCF-R3, along with 15- and 36-bp deletions (Table 1).

Combined genome-wide and transcriptome analysis

Analysis of genome-wide resequencing data yielded 419 mutation sites, mostly caused by X-ray treatment. Not all of them were related to furfural tolerance. Thus, the genome-wide and transcriptome data were combined, and 32 mutation sites related to furfural tolerance were screened from 419 mutation sites. The results of KEGG annotation classified the 32 mutation sites into three categories: transcription and translation pathways (10 sites, Schedule 3); cell function (five sites, Schedule 4); and cell metabolism (17 sites, Schedule 5). Among the five mutation sites related to cell function, *HXT1* and *TPK3* expression changed under furfural stress. Among the 17 mutation sites related to cell metabolism, *PDC6*, *MAE1*, *ZWF1*, *GAL7*, and *TDA10* are involved in carbohydrate metabolism, *OLE1* is related to lipid metabolism, and *LAT1* regulates energy production and conversion. The other major genes included *GND2* and *ZWF1*, which participate in carbohydrate metabolism and other amino acid metabolism, *ACO2*, which participates in cofactor/vitamin metabolism and cell growth/death, *TDA10*, which participates in carbohydrate, amino acid, and lipid metabolism, and *ALD5*, which participates in carbohydrate, amino acid, lipid, cofactor, and vitamin metabolism (Table 2).

Analysis of RT-qPCR results

The 32 mutation sites related to furfural tolerance were either SNPs or InDels induced by X-ray radiation plus ALE (Fig. 7a). RT-qPCR was used to verify the mutation sites of *GAL7, MAE1, PDC6, TDA10, SOL4, HXT1, TPK3, ACO2, AUS1, ALD5, LAT1*, and *GND2.* Nine of these genes, *GAL7, MAE1, PDC6, TDA10, SOL4, HXT1, TPK3, AUS1*, and *ALD5*, were all up-regulated under furfural stress (Fig. 7b). In particular, the gene encoding pyruvate decarboxylase (*PDC6*) was up-regulated ninefold compared to its WT levels. *PDC6* participates in

Table 1 Statistics of insertion and deletion fragment length

	Insertion				Deletion			
	SCF-R1	SCF-R2	SCF-R3	SCF-R4	SCF-R1	SCF-R2	SCF-R3	SCF-R4
1 bp	41	28	45	44	76	72	75	82
2 bp	9	9	6	7	39	36	25	44
3 bp	0	1	1	0	4	5	2	6
4 bp	1	1	1	2	0	0	1	0
5 bp	0	0	0	0	0	0	0	1
6 bp	1	0	0	0	0	0	0	0
7 bp	1	0	0	0	0	0	0	0
8 bp	0	1	0	1	0	0	1	0
9 bp	0	0	0	0	0	0	0	0
10 bp	1	0	0	0	0	0	0	0
15 bp	0	0	0	0	0	0	1	0
29 bp	1	0	0	0	0	0	0	0
36 bp	0	0	0	0	1	1	1	0
45 bp	1	1	1	0	0	0	0	0
97 bp	1	0	0	0	0	0	0	0

Table 2 Mutation sites related to the improvement of furfural tolerance of *S. cerevisiae*

System name	Standard name	FPKM	log2FC	Description
YOR341W	RPA190	140.83	1.58	RNA polymerase A
YJR063W	RPA12	229.45	4.64	RNA polymerase I subunit A12.2
YNL112W	DBP2	1399.74	4.67	ATP-dependent RNA helicase
YHR094C	HXT1	237.18	3.35	Low-affinity glucose transporter
YKL166C	TPK3	75.28	1.76	cAMP-dependent protein kinase catalytic subunit
YGR087C	PDC6	0.97	2.12	Minor isoform of pyruvate decarboxylase
YKL029C	MAE1	118.05	2.60	Mitochondrial malic enzyme
YNL241C	ZWF1	155.20	−1.35	Glucose-6-phosphate dehydrogenase
YBR018C	GAL7	2.40	−2.08	Galactose-1-phosphate uridyl transferase
YGR205W	TDA10	20.11	−2.75	ATP-binding protein
YGL055W	OLE1	1916.41	1.99	Delta(9) fatty acid desaturase
YNL071W	LAT1	4.82	2.39	Dihydrolipoamide acetyltransferase component
YER073W	ALD5	190.66	3.85	Mitochondrial aldehyde dehydrogenase
YGR256W	GND2	3.82	−2.69	6-Phosphogluconate dehydrogenase
YGR248W	SOL4	14.40	4.25	6-Phosphogluconolactonase

the catabolism of aromatic acid, alanine, and tryptophan, and is related to ethanol formation [36]. Additionally, *GAL7* expression (encoding galactose) increased fivefold, while *TPK3*, a gene involved in regulating mitochondrial ROS production, increased fourfold [37]. The expression of *AUS1*, a plasma membrane ATP-binding cassette transporter in *S. cerevisiae* that participates in sterol input, also increased fourfold [38].

The increased expression of these mutation sites under furfural stress indicated that they are involved in the mechanism underlying furfural tolerance. A network diagram of these genes confirmed that their interaction improved furfural resistance in *S. cerevisiae* (Fig. 7c).

Evaluation of fermentation performance of mutant strains and the WT strain under furfural stress

The fermentation abilities of the four mutant strains were compared with WT after adding 3.5 g/L furfural to the fermentation medium (Fig. 8). Glucose consumption did not differ between the five strains after furfural stress for 24 h and 48 h, indicating that the cells were arrested during this period (Fig. 8a). However, after 48 h, the glucose consumption rate of the four mutant strains accelerated. After 72 h, the glucose consumption of mutant SCF-R4 was 1.16, 1.11, and 1.08 times that of SCF-R1, SCF-R2, and SCF-R3, respectively, as well as 1.9 times that of WT. Thus, SCF-R4 exhibited enhanced carbon utilization under furfural stress.

Simultaneously, ethanol production was measured across the five strains after 24, 48, 72, and 96 h under furfural stress (Fig. 8b). After fermenting for 96 h in a fermentation broth containing 200 g/L glucose, the ethanol production of mutant SCF-R4 was 80.7 g/L, while the ethanol production of SCF-R3, SCF-R2, SCF-R1, and WT were 78.4, 76.5, 73.5, and 43.3 g/L, respectively. Thus, SCF-R4 had 1.10, 1.06, 1.03, and 1.86 times the yield of SCF-R1, SCF-R2, SCF-R3, and WT, respectively.

Discussion

Enhancing the tolerance of brewing yeast to inhibitors in lignocellulosic hydrolysates is crucial for ethanol bioproduction. In this study, a new strategy was developed to cultivate mutant strains of brewing yeast with increased tolerance to high furfural stress. Ionizing radiation was utilized to enhance genetic diversity in strains, then ALE was used under furfural stress conditions to screen for mutants with improved furfural tolerance. As previous research has shown, combining ionizing radiation with ALE can yield satisfactory breeding outcomes. Liu et al. [39] combined ALE and atmospheric room temperature plasma, enhancing the probiotic characteristics of *Bacillus coagulans*. Kato et al. [40] used carbon ion radiation and ALE to obtain mutants with 7% tolerance to salt stress. Wu et al. [41] used nitrogen ions and gamma rays in combination with ALE, significantly improving the substrate tolerance, biomass, and menadione yield of the target strain. In this study, four mutants that were resistant to high concentrations of furfural, named SCF-R1, SCF-R2, SCF-R3, and SCF-R4, were obtained through the proposed breeding strategy. These mutants exhibited furfural tolerance at concentrations of 4.0, 4.2, 4.4, and 4.5 g/L, respectively. By conducting physiological and biochemical analyses, subcellular structure examinations, RNA-seq, and whole-genome resequencing on the four mutant strains, insights into the mechanisms associated with their improved furfural tolerance were obtained.

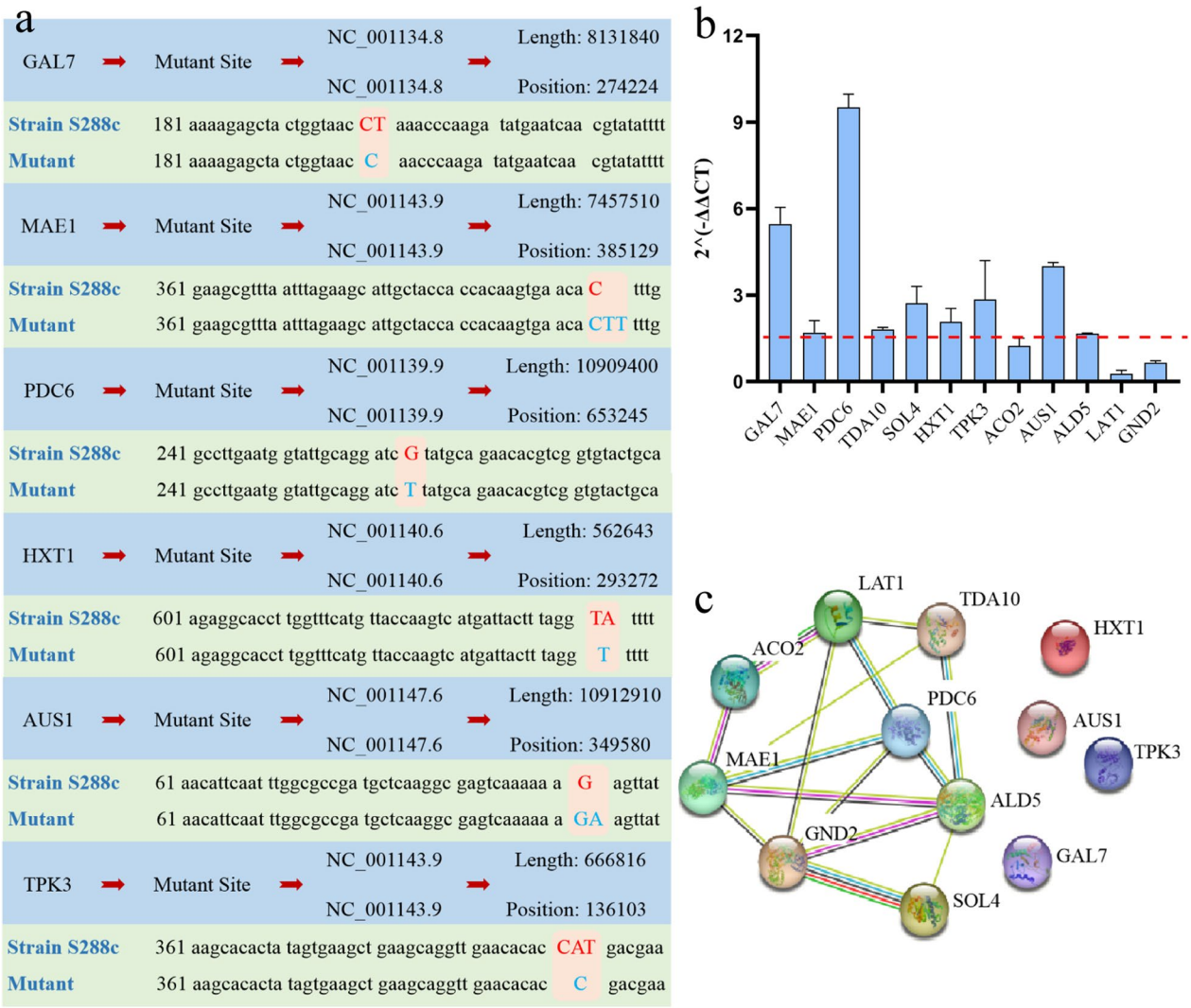

Fig. 7 Verification and analysis of mutation sites related to improving the furfural tolerance of *Saccharomyces cerevisiae*. **a** Mutation sequence characteristics of mutation sites; **b** fluorescence quantitative PCR verification results of the mutation sites; **c** interaction network diagram of the mutation sites. The fluorescence quantitative PCR results are the average of three experiments. PCR, polymerase chain reaction

The growth and fermentation performance of four mutant strains were studied in the presence of 3.5 g/L furfural; the growth performance of the four mutant strains was superior to that of the WT strain. Moreover, the mutant strain SCF-R4 had a lag phase of 36 h, while the WT strain had a lag phase of 60 h, demonstrating that the mutation significantly shortened the lag phase associated with furfural toxicity [42]. In the presence of 3.5 g/L furfural, after 96 h of fermentation, the four mutant strains consumed over 92% of the initial glucose, while the WT strain only consumed 64.67%, indicating that the four mutant strains utilized glucose at a faster rate [11]. Furthermore, the ethanol yield of the four mutant strains after 96 h of fermentation was significantly higher than that of the WT strain, with the mutant strain SCF-R4 producing ethanol at 1.86 times the yield of the WT strain, greatly increasing ethanol production under furfural stress. Compared to the WT strain, the four mutant strains showed improved furfural tolerance, demonstrating better growth performance and higher fermentation efficiency.

The enhancement of furfural tolerance in the mutant strains may be associated with changes in subcellular structure or function. Previous studies have shown that furfural toxicity destroys cell membrane integrity, resulting in mitochondrial dysfunction and ROS accumulation [7]. In this study, the four mutant strains had significantly lower MDA content than the WT strain

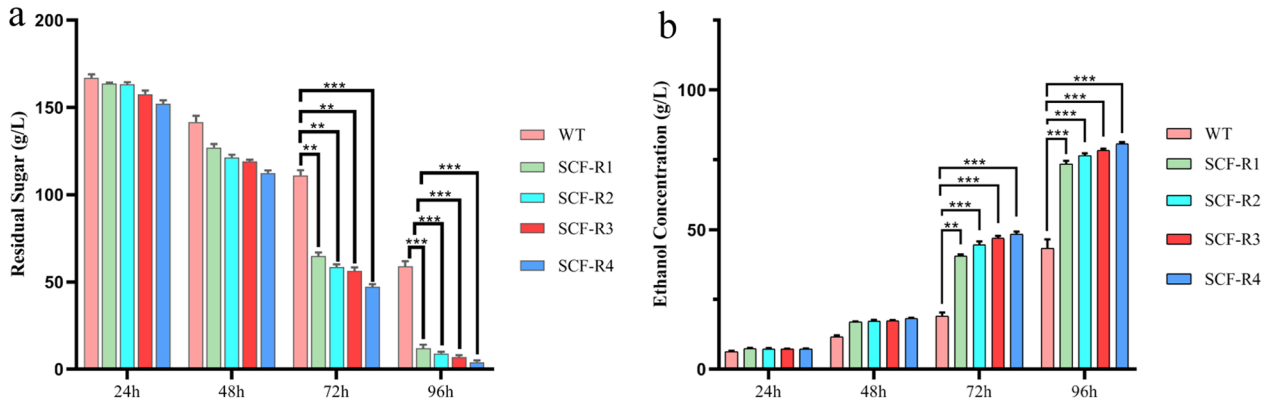

Fig. 8 Comparison of the ethanol production ability between four mutant strains tolerant to high furfural stress and the WT strain. **a** The ability of four mutant strains and the WT strain to utilize glucose at 3.5 g/L furfural; **b** the ethanol production by four mutant strains and the WT strain at 3.5 g/L furfural. The results shown are the average of three experiments. WT, wild-type

under furfural stress. The intracellular MDA content of mutant SCF-R4 was particularly low, indicating that longer radiation times appeared to have selected for stronger cell membranes, resulting in mutant strains that tolerated higher furfural stress. Change in the MMP is a key index for evaluating mitochondrial functional integrity [43–46]. Furfural stress can decrease the MMP of *S. cerevisiae* and increase mitochondrial membrane permeability, leading to mitochondrial function loss and cell death [7, 47, 48]. In line with existing research, the MMP of the four mutant strains in this study did not decrease significantly under furfural stress, whereas the WT MMP did, implying that mitochondrial function was important for *S. cerevisiae* to resist furfural toxicity and maintain cell function.

In addition to loss of mitochondrial function, furfural stress causes excessive ROS accumulation that eventually results in DNA and protein damage, as well as programmed cell death [7, 49, 50]. The ROS content of the WT was significantly higher than that of the four mutant strains under furfural stress, consistent with previous research [12]. The findings of this study indicate that the four mutant strains were either able to limit ROS accumulation or possessed ROS-scavenging capacity. The latter is mainly mediated by *SOD1, SOD2, CTT1*, and *GSH1* [51–53]. However, comparative analysis of transcriptome data after furfural stress showed that these genes were down-regulated. Therefore, in this study, the mutant strains may alleviate furfural-induced oxidative stress injury by limiting ROS production rather than through ROS scavenging [37].

The four mutants exhibited shorter lag periods than the WT strain under furfural stress, while also having high activity. This was particularly noticeable for mutant strain SCF-R4. This pattern corroborates the intracellular ROS data obtained in this study. Overall, it is speculated that the improvement of cell membrane integrity, stable mitochondrial function, and the ability to limit ROS production are the primary reasons for the elevated tolerance to high furfural concentrations.

The enhancement of furfural tolerance in the mutant strains is closely related to changes at the genetic level. Ionizing radiation greatly increases genetic diversity through single nucleotide mutations, changes in genome copy number, gene amplification, rearrangement, and deletions [54]. In this study, the mutants had numerous mutation sites, including SNPs and some small InDels. Notably, the base conversion and transversion ratios of SCF-R1, SCF-R2, SCF-R3, and SCF-R4 were 0.464, 0.194, 0.167, and 0.129, respectively. Previous studies have shown that the Ti/Tv from ionizing radiation is 0.746 [35], the Ti/Tv from spontaneous mutation is 1.12 [55], and the Ti/Tv from chemical mutation is < 1 [56]. Hence, for the furfural-tolerant mutants in this study, Ti/Tv gradually decreased with increasing radiation duration, indicating that the transformation frequency was higher than the transversion frequency. In addition, ionizing radiation can induce double-strand breaks and cluster damage in cells [57, 58], theoretically leading to a structural variant (SV). However, few studies are available on large SVs in mutant strains induced by ionizing radiation or other mutagens, likely because most DNA damage can be repaired by DNA damage response pathways [59, 60], and large SVs are difficult to pass on to offspring [61, 62]. As a result, the main mutation types in most mutant genomes are SNPs and small InDels, and the ratio of large InDels to SNPs is very low [63]. Interestingly, however, numerous large InDels were found in the four mutant strains in this study (e.g., 6, 7, 10, 29, 45, and 97-bp insertions and 36-bp deletions). The

mutation sites of these large fragments were traced in the transcriptome after furfural stress. They were found to be enriched in transcription/translation pathways, encoding the formation of mutant cytoplasm proteins with unknown functions. Therefore, large InDels may be a special molecular mechanism resulting from the proposed procedure of multi-round X-ray progressive radiation plus ALE.

To further understand the detailed genetic mechanism of furfural tolerance, 32 relevant mutations were screened, and they were found to be related to cell metabolism, transcription, translation, and cell function. Therefore, it is speculated that the mutations induced via the proposed strategy enhanced the function of these specific genes, and the resultant physiological changes improved the furfural tolerance of the yeast cells. Verification with RT-qPCR confirmed this hypothesis. For example, research on the galactose/glucose-metabolism gene *GAL7* [64] suggests that yeast cells accelerate carbon source transport under furfural stress, providing energy for cells to resist furfural-related damage [65]. *MAE1* encodes the malic enzyme, a mitochondrial enzyme that can convert malic acid into pyruvate [66] and produce NADPH, which can reduce furfural to furfuryl alcohol [67]. Likewise, *PDC6* encodes pyruvate decarboxylase, which participates in the catabolism of aromatic acids, alanine, and tryptophan, while also being related to ethanol formation in *S. cerevisiae* [36, 67]. This link could explain why the ethanol production of the four mutant strains was higher than that of the WT under furfural stress. *HXT1* encodes a glucose transporter [68] that accelerates glucose movement and promotes ATP formation in cells, both of which are beneficial to growth in high furfural concentrations. *AUS1* encodes an ATP-based plasma membrane sterol transporter that incorporates sterols into the plasma membrane to form ergosterol [38]. This major component of microbial cells is critical to ensuring cell membrane integrity, membrane-bound enzyme activity, membrane fluidity, cell viability, and material transportation. The addition of exogenous ergosterol under furfural stress shortened the lag period of *S. cerevisiae* by 50%, increased ethanol production by 158%, decreased intracellular ROS by 53%, and decreased cell membrane porosity [69]. Finally, *TPK3* encodes a cAMP-dependent protein kinase that regulates mitochondrial biogenesis [37]. The cAMP signaling pathway is closely related to mitochondria content. In particular, Tpk3p-induced cAMP-dependent phosphorylation regulates respiratory chain complexes related to the ROS production rate; thus, when Tpk3p is highly expressed, the mitochondrial ROS content decreases [70]. Therefore, it is suspected that *TPK3* mutation and up-regulation may limit mitochondrial ROS production, significantly lowering oxidative stress in mutant strains and benefiting furfural tolerance.

Conclusions

This study proposes that multiple rounds of X-ray progressive radiation combined with ALE is an efficient strategy to produce desired mutant strains. Using this strategy, four significantly improved furfural-tolerant brewing yeast mutants, SCF-R1, SCF-R2, SCF-R3, and SCF-R4, were selected through four rounds of processing. The mechanism of furfural tolerance was also identified. Specifically, the mutants are able to improve their cell membrane integrity, stabilize mitochondrial function, and limit ROS production under furfural stress to enhance furfural tolerance. Transcriptome and genome-wide analysis revealed that the four mutant strains had numerous mutation sites, mostly comprising InDels, suggesting that this form of mutation may be a mechanism for rapidly adjusting to adverse environments. Furthermore, 32 mutation sites (genes) related to the improvement of furfural tolerance in *S. cerevisiae* were screened. The identification of these genes will benefit future investigations of the genetic mechanism of furfural tolerance. In conclusion, this work provides valuable insight on the evolution of furfural stress tolerance in *S. cerevisiae* and offers empirical evidence of the proposed method's feasibility. The ability to rapidly breed new toxicity-tolerant strains with applications in biofuels should greatly aid in the development of sustainable energy.

Limitations, policy implications, and future prospects

(1) The current study has the following limitations:

a. Technical challenges: The use of multi-round gradual X-ray radiation combined with adaptive laboratory evolution to screen for yeast mutant strains tolerant to furfural stress may face limitations owing to the complexity of the technical operations involved and cost constraints.

b. Validation of mutation sites: Exploring mutation sites related to the enhancement of furfural tolerance in yeast mutants may be restricted by technical means, requiring more precise gene editing technology to accurately identify relevant sites.

c. Experimental verification: Research results need to be validated in actual industrial production environments to ensure the feasibility and effectiveness of translation into practical applications.

(2) Policy implications:

The research findings provide theoretical support for improving the furfural tolerance of yeast strains, further driving the development of second-generation bioethanol production from lignocellulosic biomass.

(3) Future prospects:

a. Further optimization of experimental protocols and technical methods can enhance the efficiency and accuracy of screening yeast mutant strains tolerant to furfural stress, expanding the depth and breadth of this research.

b. By integrating emerging bioinformatics technologies, the in-depth exploration of combined transcriptome and genome mining can be conducted to discover more potential mutation sites related to improving furfural tolerance in yeast, accelerating the translation and application of research findings.

c. By aligning with industry demands, exploring the potential applications of research findings in actual production settings can drive the transformation of scientific research outcomes into industrial applications, promoting technological innovation and industrial development in relevant fields.

Methods

Original strain culture

S. cerevisiae S288c was selected as the starting strain. Fresh medium was prepared by mixing 2% agar with solid YPD medium (2% glucose, 2% peptone, and 1% yeast extract). Frozen *S. cerevisiae* cells were inoculated in fresh YPD medium, cultured at 30 °C and 200 rpm until the OD_{600} was 0.6–0.8 (logarithmic growth period), and then transferred twice to obtain high-viability strains.

Radiation treatment and ALE

Cell suspensions of high-viability strains were inoculated into 33-mm culture dishes, and sample thickness was controlled to approximately 2.5 mm. The samples were irradiated at a dose of 120 Gy [71], then repaired at 10 mL YPD for 6–10 h. Rehabilitated strains were inoculated in fresh YPD medium containing 2.0 g/L furfural at 4% inoculum and acclimated using an ALE gradient. Specifically, this procedure involved transferring surviving yeast cells at the logarithmic growth stage to fresh YPD medium containing a higher furfural concentration, then transferring them ten more times within 72 h until the $OD_{600} < 0.2$, when acclimation ended. Re-irradiation was then performed, and the process was repeated (Fig. 9).

Growth and fermentation in furfural culture

The WT and four mutant strains were inoculated into fresh YPD medium (100 mL) until they reached the logarithmic phase (identical OD_{600} values). Next, they were cultured in YPD medium containing 3.5 g/L furfural at 4% inoculum, under conditions of 200 rpm and 30 ℃. Their growth curves were drawn after measuring OD values at 600 nm every 12 h. The five strains were also inoculated into a fermentation medium (20% glucose, 2% peptone, 1% yeast) containing 3.5 g/L furfural at 8% inoculum. The ethanol and residual sugar content were determined at 24, 48, 72, and 96 h. Three biological repeats were performed per sample.

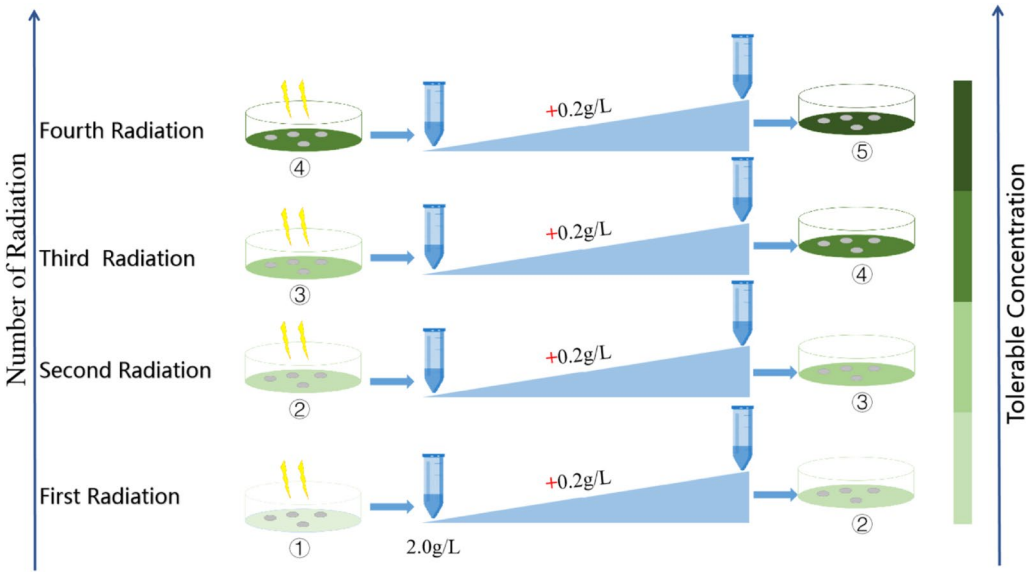

Fig. 9 Schematic diagram of multiple rounds of progressive X-ray radiation combined with ALE

Measuring MDA, MMP, and ROS in furfural culture

For the stress experiments, 3.5 g/L furfural was added to WT and mutant strains at the logarithmic stage. Cells were centrifuged after 0 and 3 h of stress, then washed with ice-cold phosphate-buffered saline (PBS). After obtaining the crude enzyme solution through lysis, it was placed on ice and the thiobarbituric acid reagent from the Solarbio MDA assay kit was used to determine the cellular MDA content [72]. Determining the MDA is a common method for measuring lipid peroxidation [59]. Intracellular levels of ROS were measured with the DCFH-DA probe in an ROS detection kit (Solarbio, Beijing, China) and the MMP was measured using Rhodamine 123 [73, 74]. Each sample was subjected to three biological repeats.

RNA extraction and transcriptome sequencing

When exposed to high concentrations of furfural for a short period, yeast may quickly initiate stress response mechanisms, leading to changes in gene expression levels. Transcriptomic sequencing analysis can better elucidate the gene expression regulation patterns associated with early responses to furfural stress. Therefore, after 2 h of stress treatment with 30 g/L furfural, three *S. cerevisiae* samples at the logarithmic stage were washed twice with PBS, frozen in liquid nitrogen, and transferred to an ultra-low temperature refrigerator. Total RNA was obtained using an RNA extraction and purification kit (Sangon Biotech) [75], quantified using a Nanodrop 2000, and visualized with agarose gel electrophoresis using an Agilent 2100 instrument. Total RNA ($OD_{260/280} > 1.8$ and $OD_{260/230} > 2.0$) were used for sequencing. Gene-expression fold changes between the stress and control groups were calculated based on three fragments per kilobase million values per gene [76]. The detection thresholds of DEGs were q-value ≤ 0.01 and fold change ≥ 2. Corresponding p values were also determined [75].

Genome-wide analysis and RT-qPCR verification

The four mutant strains and one WT strain underwent five successive subcultures. Cells were collected at the logarithmic phase (OD_{600}: 0.6–0.8) for total DNA extraction using the E.Z.N.A Yeast DNA Extraction Kit [77]. Whole genome sequencing was performed using an Illumina HiSeq™ X10. After cleaning, the sequenced data were compared with the reference genome using BWA (http://bio-bwa.sourceforge.net/bwa.shtml, v0.7.15) and SAMtools (http://www.htslib.org/workflow/#mapping_to_variant, v1.3.1). Next, functional analysis on SNPs and InDels was performed to obtain mutation sites related to furfural tolerance; the results were verified with RT-qPCR [75]. Primers were designed in Primer3 (http://frodo.wi.mit.edu/). Total RNA extraction and quality control followed the procedures described in Sect. 2.5. Complementary DNA was synthesized using the FastKing gDNA Dispelling RT SuperMix kit, and the cDNA copy number was quantified using the Rotor-Gene Q2plex system with the SYBR Green PCR kit.

Statistics

Data were analyzed in Origin 2018, GraphPad Prism 8, and SPSS 17.0 (SPSS Inc, Chicago, IL). The latter was specifically used for one-way random-effects analysis of variance and the least significant difference test. Significance was set at $p < 0.05$. Each experiment was conducted independently at least three times.

Abbreviations

ATP	Adenosine triphosphate
ALE	Adaptive laboratory evolution
SNPs	Single nucleotide polymorphisms
InDels	Insertions and deletions
WT	Wild-type
YPD	Yeast extract peptone dextrose
MDA	Malondialdehyde
MMP	Mitochondrial membrane potential
ROS	Reactive oxygen species
DCFH-DA	2,7-Dichlorodihydrofluorescein diacetate
DEGs	Differentially expressed genes
KEGG	Kyoto Encyclopedia of Genes and Genomes

Supplementary Information

The online version contains supplementary material available at https://doi.org/10.1186/s13068-024-02562-w.

Additional file 1.

Acknowledgements

Not applicable.

Author contributions

DL, XG, and JR conceived the idea and participated in revision and discussion; JR, MZ, XZ, and ND performed the data analysis; CL, CJ, YW, and JZ helped with data collection and the methods; JR, CJ, and ZD conducted the experiments; JR, MZ, and CL drafted the manuscript with the significant participation of CL. All authors read and approved the final manuscript.

Funding

This work was supported by the National Natural Science Foundation of China (Nos. 11975284, 11905265, and 12205132), the "Western Young Scholar" key project of the Chinese Academy of Sciences 2023, the Lanzhou Talent Innovation and Entrepreneurship Project (No. 2022-RC-37), and the Gansu Youth Science and Technology Fund Project (No. 22JR5RA300).

Availability of data and materials

The original sequence data reported in this paper have been stored in the China National Center for Bioinformation (registration number CRA012619), which can be publicly accessed at https://ngdc.cncb.ac.cn/.

Declarations

Ethics approval and consent to participate

Not applicable.

Consent for publication
Not applicable.

Competing interests
The authors declare no competing interests.

Author details
[1]Institute of Modern Physics, Chinese Academy of Sciences, No. 509 Nanchang Road, Lanzhou 730000, Gansu, China. [2]University of Chinese Academy of Sciences, Beijing 100049, China. [3]School of Life Science and Engineering, Lanzhou University of Technology, No. 36 Peng Jiaping, Lanzhou 730050, Gansu, China.

Received: 14 November 2023 Accepted: 9 August 2024
Published online: 22 August 2024

References

1. Patel A, Shah AR. Integrated lignocellulosic biorefinery: gateway for production of second generation ethanol and value added products. J Biores nd Bioprod. 2021;6(2):108–28. https://doi.org/10.1016/j.jobab.2021.02.001.
2. Nandhini R, Rameshwar SS, Sivaprakash B, et al. Carbon neutrality in biobutanol production through microbial fermentation technique from lignocellulosic materials-a biorefinery approach. J Clean Prod. 2023;413:137470. https://doi.org/10.1016/j.jclepro.2023.137470.
3. Wang P, Dudareva N, Morgan JA, Chapple C. Genetic manipulation of lignocellulosic biomass for bioenergy. Curr Opin Chem Biol. 2015;29:32–9. https://doi.org/10.1016/j.cbpa.2015.08.006.
4. Baig KS, Wu J, Turcotte G. Future prospects of delignification pretreatments for the lignocellulosic materials to produce second generation bioethanol. Int J Energy Res. 2019;43:1411–27. https://doi.org/10.1002/er.4292.
5. Kumar V, Yadav SK, Kumar J, Ahluwalia V. A critical review on current strategies and trends employed for removal of inhibitors and toxic materials generated during biomass pretreatment. Bioresour Technol. 2020;299: 122633. https://doi.org/10.1016/j.biortech.2019.122633.
6. Zheng YY, Kong ST, Luo SQ, Chen C, Cui Z, Sun X, et al. Improving furfural tolerance of *Escherichia coli* by integrating adaptive laboratory evolution with CRISPR-enabled trackable genome engineering (CREATE). ACS Sustain Chem Eng. 2022;10(7):2318–30. https://doi.org/10.1021/acssuschemeng.1c05783.
7. He MX, Wu B, Shui ZX, Hu QC, Wang WG, Tan FR, et al. Transcriptome profiling of *Zymomonas mobilis* under furfural stress. Appl Microbiol Biotechnol. 2012;95(1):189–99. https://doi.org/10.1007/s00253-012-4155-4.
8. Allen SA, Clark W, McCaffery JM, Cai Z, Lanctot A, Slininger PJ, et al. Furfural induces reactive oxygen species accumulation and cellular damage in *Saccharomyces cerevisiae*. Biotechnol Biofuels. 2010;3:2. https://doi.org/10.1186/1754-6834-3-2.
9. Jung YH, Kim S, Yang J, et al. Intracellular metabolite profiling of *Saccharomyces cerevisiae* evolved under furfural. Microb Biotechnol. 2017;10(2):395–404. https://doi.org/10.1111/1751-7915.1246.
10. Zaldivar J, Martinez A, Ingram LO. Effect of selected aldehydes on the growth and fermentation of ethanologenic *Escherichia coli*. Biotechnol Bioeng. 1999;65(1):24–33. https://doi.org/10.1002/(SICI)1097-0290(19991005)65:1%3c24::AID-BIT4%3e3.0.CO;2-2.
11. Shui ZX, Qin H, Wu B, Ruan ZY, Wang LS, Tan FR, et al. Adaptive laboratory evolution of ethanologenic *Zymomonas mobilis* strain tolerant to furfural and acetic acid inhibitors. Appl Microbiol Biotechnol. 2015;99:5739–48. https://doi.org/10.1007/s00253-015-6616-z.
12. Luo P, Zhang YN, Suo YK, Liao Z, Ma Y, Fu H, Wang J. The global regulator IrrE from *Deinococcus radiodurans* enhances the furfural tolerance of *Saccharomyces cerevisiae*. Biochem Eng J. 2018;136:69–77. https://doi.org/10.1016/j.bej.2018.05.009.
13. Huang SZ, Xue TL, Wang ZQ, Ma Y, He X, Hong J, et al. Furfural-tolerant *Zymomonas mobilis* derived from error-prone PCR-based whole genome shuffling and their tolerant mechanism. Appl Microbiol Biotechnol. 2018;102:3337–47. https://doi.org/10.1007/s00253-018-8817-8.
14. Shirasawa K, Hirakawa H, Nunome T, Tabata S, Isobe S. Genome-wide survey of artificial mutations induced by ethyl methanesulfonate and gamma rays in tomato. Plant Biotechnol J. 2015;14(1):51–60. https://doi.org/10.1111/pbi.12348.
15. Gao Y, Zhang MM, Zhou X, Guo X, Lei C, Li W, Lu D. Effects of carbon ion beam irradiation on butanol tolerance and production of *Clostridium acetobutylicum*. Front Microbiol. 2020;11: 602774. https://doi.org/10.3389/fmicb.2020.602774.
16. Gao Y, Zhou X, Zhang MM, Liu YJ, Guo XP, Lei CR, et al. Response characteristics of the membrane integrity and physiological activities of the mutant strain Y217 under exogenous butanol stress. Appl Microbiol Biotechnol. 2021;105(6):2455–72. https://doi.org/10.1007/s00253-021-11174-5.
17. Guo XP, Ren JL, Zhou X, Zhang M, Lei C, Chai R, et al. Strategies to improve the efficiency and quality of mutant breeding using heavy-ion beam irradiation. Crit Rev Biotechnol. 2023;2023:1–18. https://doi.org/10.1080/07388551.2023.2226339.
18. Zhou X, Yang Z, Jiang TT, Wang SY, Liang JP, Lu XH, Wang L. The acquisition of *Clostridium tyrobutyricum* mutants with improved bioproduction under acidic conditions after two rounds of heavy-ion beam irradiation. Sci Rep. 2016;6:29968. https://doi.org/10.1038/srep29968.
19. Zhang N, Jiang JC, Yang J, Wei M, Zhao J, Xu H, et al. Screening of thermotolerant yeast by low-energy ion implantation for cellulosic ethanol fermentation. Energy Sources A. 2018;40(9):1084–90. https://doi.org/10.1080/15567036.2018.1469692.
20. Xie M, Zhang XL, Hu XP, Zhang YJ, Peng DL, Li Q, Li M. Mutagenic effects of low-energy N+ ion implantation on the propamocarb-tolerance of nematophagous fungus *Lecanicillium attenuatum*. Biol Control. 2017;117:1–5. https://doi.org/10.1016/j.biocontrol.2017.08.017.
21. Portnoy VA, Bezdan D, Zengler K. Adaptive laboratory evolution - harnessing the power of biology for metabolic engineering. Curr Opin Biotechnol. 2011;22(4):590–4. https://doi.org/10.1016/j.copbio.2011.03.007.
22. Da Silveira FA, Soares DLD, Bang KW, Balbino TR, de Moura Ferreira MA, Diniz RH, et al. Assessment of ethanol tolerance of *Kluyveromyces marxianus* CCT 7735 selected by adaptive laboratory evolution. Appl Microbiol Biotechnol. 2020;104(17):7483–94. https://doi.org/10.1007/s00253-020-10768-9.
23. Li WC, Zhu JQ, Zhao X, Qin L, Xu T, Zhou X, et al. Improving co-fermentation of glucose and xylose by adaptive evolution of engineering xylose-fermenting *Saccharomyces cerevisiae* and different fermentation strategies. Renew Energy. 2019;139:1176–83. https://doi.org/10.1016/j.renene.2019.03.028.
24. Sarkar P, Mukherjee M, Goswami G, Das D. Adaptive laboratory evolution induced novel mutations in *Zymomonas mobilis* ATCC ZW658: a potential platform for co-utilization of glucose and xylose. J Indust Microbiol Biotechnol. 2020;47(3):329–41. https://doi.org/10.1007/s10295-020-02270-y.
25. Godara A, Kao KC. Adaptive laboratory evolution of β-caryophyllene producing *Saccharomyces cerevisiae*. Microb Cell Fact. 2021;20:106. https://doi.org/10.1186/s12934-021-01598-z.
26. Wallace-Salinas V, Gorwa-Grauslund MF. Adaptive evolution of an industrial strain of *Saccharomyces cerevisiae* for combined tolerance to inhibitors and temperature. Biotechnol Biofuels. 2013;6:151. https://doi.org/10.1186/1754-6834-6-151.
27. Liu ZJ, Radi MH, Mohamed ETT, et al. Adaptive laboratory evolution of *Rhodosporidium toruloides* to inhibitors derived from lignocellulosic biomass and genetic variations behind evolution. Biores Technol. 2021;333: 125171. https://doi.org/10.1016/j.biortech.2021.125171.
28. Dragosits M, Mattanovich D. Adaptive laboratory evolution - principles and applications for biotechnology. Microb Cell Fact. 2013;12:64. https://doi.org/10.1186/1475-2859-12-64.
29. Phaneuf PV, Yurkovich JT, Heckmann D, Wu M, Sandberg TE, King ZA, et al. Causal mutations from adaptive laboratory evolution are outlined by multiple scales of genome annotations and condition-specificity. BMC Genomics. 2020;21:514. https://doi.org/10.1186/s12864-020-06920-4.

30. Dragosits M, Mattanovich D. Adaptive laboratory evolution - principles and applications for biotechnology. Microb Cell Fact. 2013;12(1):64. https://doi.org/10.1186/1475-2859-12-64.
31. Sandberg TE, Salazar MJ, Weng LL, Palsson BO, Feist AM. The emergence of adaptive laboratory evolution as an efficient tool for biological discovery and industrial biotechnology. Metab Eng. 2019;56:1–16. https://doi.org/10.1016/j.ymben.2019.08.004.
32. Jiang GZ, Yang ZM, Wang Y, Yao M, Chen Y, Xiao W, Yuan Y. Enhanced astaxanthin production in yeast via combined mutagenesis and evolution. Biochem Eng J. 2020;156: 107519. https://doi.org/10.1016/j.bej.2020.107519.
33. Leavell MD, Singh AH, Kaufmann-Malaga BB. High-throughput screening for improved microbial cell factories, perspective and promise. Curr Opin Biotechnol. 2020;62:22–8. https://doi.org/10.1016/j.copbio.2019.07.002.
34. Lynch M, Sung W, Morris K, Coffey N, Landry CR, Dopman EB, et al. A genome-wide view of the spectrum of spontaneous mutations in yeast. Proc Natl Acad Sci. 2008;105(27):9272–7. https://doi.org/10.1073/pnas.0803466105.
35. Belfield EJ, Gan XC, Mithani A, Brown C, Jiang C, Franklin K, et al. Genome-wide analysis of mutations in mutant lineages selected following fast-neutron irradiation mutagenesis of *Arabidopsis thaliana*. Genome Res. 2012;22(7):1306–15. https://doi.org/10.1101/gr.131474.111.
36. Creamer DR, Hubbard SJ, Ashe MP, et al. Yeast protein kinase a isoforms: a means of encoding specificity in the response to diverse stress conditions? Biomolecules. 2022;12(7):958. https://doi.org/10.3390/biom12070958.
37. Chevtzoff C, Yoboue ED, Galinier A, Casteilla L, Daignan-Fornier B, Rigoulet M, Devin A. Reactive oxygen species-mediated regulation of mitochondrial biogenesis in the yeast *Saccharomyces cerevisiae*. J Biol Chem. 2009;285(3):1733–42. https://doi.org/10.1074/jbc.M109.019570.
38. Papay M, Klein C, Hapala I, Petriskova L, Kuchler K, Valachovic M. Mutations in the nucleotide-binding domain of putative sterol importers Aus1 and Pdr11 selectively affect utilization of exogenous sterol species in yeast. Yeast. 2020;37(1):5–14. https://doi.org/10.1002/yea.3456.
39. Liu KY, Fang H, Cui FJ, Nyabako BA, Tao T, Zan X, et al. ARTP mutation and adaptive laboratory evolution improve probiotic performance of *Bacillus coagulans*. Appl Microbiol Biotechnol. 2020;104(14):6363–73. https://doi.org/10.1007/s00253-020-10703-y.
40. Kato Y, Ho SH, Vavricka CJ, Chang JS, Hasunuma T, Kondo A. Evolutionary engineering of salt-resistant *Chlamydomonas* sp. strains reveals salinity stress-activated starch-to-lipid biosynthesis switching. Bioresour Technol. 2017;245:1484–90. https://doi.org/10.1016/j.biortech.2017.06.035.
41. Wu HF, Wang H, Wang P, Zhao G, Liu H, Wang L, et al. Gradient radiation breeding and culture domestication of menaquinone producing strains. Bioprocess Biosyst Eng. 2021;44(7):1373–82. https://doi.org/10.1007/s00449-021-02508-8.
42. Bhavana BK, Sandeep NM, Bokade VV, Debnath S. Effect of furfural, acetic acid and 5-hydroxymethylfurfural on yeast growth and xylitol fermentation using *Pichia stipitis NCIM 3497*. Biomass Convers Biorefin. 2024;14:4909–23. https://doi.org/10.1007/s13399-022-02758-w.
43. Martin DB, David GN. Assessing mitochondrial dysfunction in cells. Biochem J. 2011;435(2):297–312. https://doi.org/10.1042/BJ20110162.
44. Birket MJ, Orr AL, Gerencser AA, Madden DT, Vitelli C, Swistowski A, et al. A reduction in ATP demand and mitochondrial activity with neural differentiation of human embryonic stem cells. J Cell Sci. 2011;124(3):348–58. https://doi.org/10.1242/jcs.072272.
45. Lopez PC, Peng C, Arneborg N, Junicke H, Gernaey KV. Analysis of the response of the cell membrane of *Saccharomyces cerevisiae* during the detoxification of common lignocellulosic inhibitors. Sci Rep. 2021;11(1):6853. https://doi.org/10.1038/s41598-021-86135-z.
46. Upadhyay TK, Trivedi R, Khan F, Al-Keridis LA, Pandey P, Sharangi AB, et al. In vitro elucidation of antioxidant, antiproliferative, and apoptotic potential of yeast-derived β-1,3-glucan particles against cervical cancer cells. Front Oncol. 2022;12: 942075. https://doi.org/10.3389/fonc.2022.942075.
47. Kim D, Hahn JS. Roles of the Yap1 transcription factor and antioxidants in *Saccharomyces cerevisiae*'s tolerance to furfural and 5-hydroxymethylfurfural, which function as thiol-reactive electrophiles generating oxidative stress. Appl Environ Microbiol. 2013;79(16):5069–77. https://doi.org/10.1128/AEM.00643-13.
48. Wu D, Wang DM, Hong J. Effect of a novel alpha/beta hydrolase domain protein on tolerance of *K. marxianusto* lignocellulosic biomass derived inhibitors. Front Bioeng Biotechnol. 2020;8:884. https://doi.org/10.3389/fbioe.2020.00844.
49. Jilani SB, Dev C, Eqbal D, Jawed K, Prasad R, Yazdani SS. Deletion of pgi gene in *E. coli* increases tolerance to furfural and 5-hydroxymethyl furfural in media containing glucose–xylose mixture. Microb Cell Fact. 2020;19(1):153. https://doi.org/10.1186/s12934-020-01414-0.
50. Li B, Liu N, Zhao X. Response mechanisms of *Saccharomyces cerevisiae* to the stress factors present in lignocellulose hydrolysate and strategies for constructing robust strains. Biotechnol Biofuels. 2022;15(1):28. https://doi.org/10.1186/s13068-022-02127-9.
51. Qi YH, Qin QJ, Liao GY, et al. Unveiling the super tolerance of Candida nivariensis to oxidative stress: insights into the involvement of a catalase. Microbiol Spectr. 2024;12(2):e03169-e3223. https://doi.org/10.1128/spectrum.03169-23.
52. Nishimoto T, Furuta M, Kataoka M, Kishida M. Important role of catalase in the cellular response of the budding yeast *Saccharomyces cerevisiae* exposed to ionizing radiation. Curr Microbiol. 2015;70(3):404–7. https://doi.org/10.1007/s00284-014-0733-2.
53. Raghavendran V, Marx C, Olsson L, Bettiga M. The protective role of intracellular glutathione in *Saccharomyces cerevisiae* during lignocellulosic ethanol production. AMB Express. 2020;10(1):219. https://doi.org/10.1186/s13568-020-01148-7.
54. Ma LQ, Kong FQ, Sun K. From classical radiation to modern radiation: past, present, and future of radiation mutation breeding. Front Public Health. 2021;9: 768071. https://doi.org/10.3389/fpubh.2021.768071.
55. Ossowski S, Schneeberger K, Lucas-Lledó JI, Warthmann N, Clark RM, Shaw RG, et al. The rate and molecular spectrum of spontaneous mutations in *Arabidopsis thaliana*. Science. 2010;327(5961):92–4. https://doi.org/10.1126/science.1180677.
56. Mladenova V, Mladenov E, Stuschke M, Iliakis G. DNA damage clustering after ionizing radiation and consequences in the processing of chromatin breaks. Molecules. 2022;27(5):1540. https://doi.org/10.3390/molecules27051540.
57. Kamp GVD, Heemskerk T, Kanaar R, Essers J. DNA double strand break repair pathways in response to different types of ionizing radiation. Front Genet. 2021;12: 738230. https://doi.org/10.3389/fgene.2021.738230.
58. Terato H, Tanaka R, Nakaarai Y, Nohara T, Doi Y, Iwai S, et al. Quantitative analysis of isolated and clustered DNA damage induced by gamma-rays, carbon ion beams, and iron ion beams. J Radiat Res. 2008;40(2):133–46. https://doi.org/10.1269/jrr.07089.
59. Santivasi WL, Xia F. Ionizing radiation-induced DNA damage, response, and repair. Antioxid Redox Signal. 2014;21(2):251–9. https://doi.org/10.1089/ars.2013.5668.
60. Zhang MM, Cao GZ, Guo XP, Gao Y, Li W, Lu D. A comet assay for DNA damage and repair after exposure to carbon-ion beams or X-rays in *Saccharomyces cerevisiae*. Dose Response. 2018;16(3):1–9. https://doi.org/10.1177/1559325818792467.
61. Du Y, Luo SW, Li X, Yang J, Cui T, Li W, et al. Identification of substitutions and small insertion-deletions induced by carbon-ion beam irradiation in *Arabidopsis thaliana*. Front Plant Sci. 2017;8:1851. https://doi.org/10.3389/fpls.2017.01851.
62. Naito K, Kusaba M, Shikazono N, Takano T, Tanaka A, Tanisaka T, et al. Transmissible and nontransmissible mutations induced by irradiating *Arabidopsis thaliana* pollen with γ-rays and carbon ions. Genetics. 2005;169(2):881–9. https://doi.org/10.1534/genetics.104.033654.
63. Kazama Y, Ishii K, Hirano T, Wakana T, Yamada M, Ohbu S, Abe T. Different mutational function of low-and high-linear energy transfer heavy-ion irradiation demonstrated by whole-genome resequencing of Arabidopsis mutants. Plant J. 2017;92(6):1020–30. https://doi.org/10.1111/tpj.13738.
64. Lu R, Shi TQ, Lin L, Ledesma-Amaro R, Ji XJ, Huang H. Advances in metabolic engineering of yeasts for the production of fatty acid-derived hydrocarbon fuels. Green Chem Eng. 2022;3(4):289–303. https://doi.org/10.1016/j.gce.2022.07.008.
65. Paes BG, Steindorff AS, Formighieri EF, et al. Physiological characterization and transcriptome analysis of Pichia pastoris reveals its response to lignocellulose-derived inhibitors. AMB Expr. 2021;11:2. https://doi.org/10.1186/s13568-020-01170-9.
66. Zhang NN, Wang FE, Nwamba MC, et al. Enhancing tolerance of *Kluyveromyces marxianus* to lignocellulose-derived inhibitors and its

ethanol production from corn cob via overexpression of a nitroreductase gene. Ind Crops Prod. 2024;203: 117136. https://doi.org/10.1016/j.indcrop.2023.117136.
67. Zeng LJ, Huang JX, Feng PX, et al. Transcriptomic analysis of formic acid stress response in *Saccharomyces cerevisiae*. World J Microbiol Biotechnol. 2022;38:34. https://doi.org/10.1007/s11274-021-03222-z.
68. Ding J, Bierma J, Smith MR, Poliner E, Wolfe C, Hadduck AN, et al. Acetic acid inhibits nutrient uptake in *Saccharomyces cerevisiae*: auxotrophy confounds the use of yeast deletion libraries for strain improvement. Appl Microbiol Biotechnol. 2013;97(16):7405–16. https://doi.org/10.1007/s00253-013-5071-y.
69. Jia YP, Zhang QY, Dai J, Zheng X, Meng X, Zhou R, et al. Ergosterol supplementation improves furfural tolerance of *Saccharomyces cerevisiae* to produce ethanol and its underlying mechanism. BioResources. 2023;18(1):228–46. https://doi.org/10.15376/biores.18.1.228-246.
70. Bouchez C, Devin A. Mitochondrial biogenesis and mitochondrial reactive oxygen species (ROS): a complex relationship regulated by the cAMP/PKA signaling pathway. Cells. 2019;8(4):287. https://doi.org/10.3390/cells8040287.
71. Ma YB, Wang ZY, Zhu M, Yu C, Cao Y, Zhang D, Zhou G. Increased lipid productivity and TAG content in *Nannochloropsis* by heavy-ion irradiation mutagenesis. Bioresour Technol. 2013;136C(136):360–7. https://doi.org/10.1016/j.biortech.2013.03.020.
72. Xiao HW, Li Y, Luo D, Dong JL, Zhou LX, Zhao SY, et al. Hydrogen-water ameliorates radiation-induced gastrointestinal toxicity via MyD88's effects on the gut microbiota. Exp Mol Med. 2018;50: e433. https://doi.org/10.1038/emm.2017.246.
73. Zhang J, Ahmad S, Wang LY, Han Q, Zhang JC, Luo YP. Cell death induced by α-terthienyl via reactive oxygen species-mediated mitochondrial dysfunction and oxidative stress in the midgut of *Aedes aegypti* larvae. Free Radic Biol Med. 2019;137:87–98. https://doi.org/10.1016/j.freeradbiomed.2019.04.021.
74. Porro D, Smeraldi C, Martegani E, Ranzi BM, Alberghina L. Flow-cytometric determination of the respiratory activity in growing *Saccharomyces cerevisiae* populations. Biotechnol Prog. 1994;10(2):193–7. https://doi.org/10.1021/bp00026a009.
75. Guo XP, Zhang MM, Gao Y, Lu D, Li W, Zhou L. Repair characteristics and time dependent effects in response to heavy-ion beam irradiation in *Saccharomyces cerevisiae*: a comparison with X-ray irradiation. Appl Microbiol Biotechnol. 2020;104(9):4043–57. https://doi.org/10.1007/s00253-020-10464-8.
76. Trapnell C, Williams BA, Pertea G, Mortazavi A, Kwan G, Van Baren MJ, et al. Transcript assembly and quantification by RNA Seq reveals unannotated transcripts and isoform switching during cell differentiation. Nat Biotechnol. 2010;28(5):511–5. https://doi.org/10.1038/nbt.1621.
77. Guo XP, Zhang MM, Gao Y, Cao G, Yang Y, Lu D, Li W. A genome-wide view of mutations in respiration-deficient mutants of *Saccharomyces cerevisiae* selected following carbon ion beam irradiation. Appl Microbiol Biotechnol. 2019;103(4):1851–64. https://doi.org/10.1007/s00253-019-09626-0.

Publisher's Note